

# ChemComm

Accepted Manuscript



This article can be cited before page numbers have been issued, to do this please use: G. Chen, C. Chen, X. Li, H. Ma and Y. Dong, *Chem. Commun.*, 2018, DOI: 10.1039/C8CC07208F.



This is an Accepted Manuscript, which has been through the Royal Society of Chemistry peer review process and has been accepted for publication.

Accepted Manuscripts are published online shortly after acceptance, before technical editing, formatting and proof reading. Using this free service, authors can make their results available to the community, in citable form, before we publish the edited article. We will replace this Accepted Manuscript with the edited and formatted Advance Article as soon as it is available.

You can find more information about Accepted Manuscripts in the [author guidelines](#).

Please note that technical editing may introduce minor changes to the text and/or graphics, which may alter content. The journal's standard [Terms & Conditions](#) and the ethical guidelines, outlined in our [author and reviewer resource centre](#), still apply. In no event shall the Royal Society of Chemistry be held responsible for any errors or omissions in this Accepted Manuscript or any consequences arising from the use of any information it contains.



Journal Name

COMMUNICATION

## Cu<sub>3</sub>L<sub>2</sub> metal-organic cage for A<sup>3</sup>-coupling reaction: reversible coordination interaction triggered homogeneous catalysis and heterogeneous recovery

Received 00th January 20xx,  
Accepted 00th January 20xx

DOI: 10.1039/x0xx00000x

Gong-Jun Chen, Chao-Qun Chen, Xue-Tian Li, Hui-Chao Ma, and Yu-Bin Dong\*

www.rsc.org/

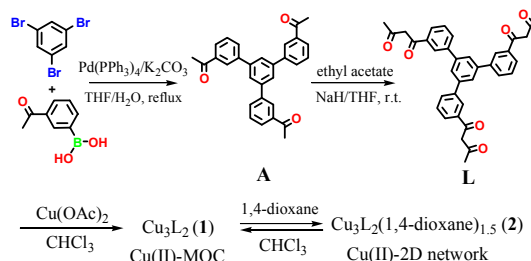
The reported Cu(II) metal-organic cage (Cu<sub>3</sub>L<sub>2</sub>, **1**) can be a highly active reusable catalyst to homogeneously catalyze the A<sup>3</sup>-coupling reaction in CHCl<sub>3</sub> and can be heterogeneously recovered by simply addition of 1,4-dioxane via formation of the insoluble metal-organic framework (Cu<sub>3</sub>L<sub>2</sub>(1,4-dioxane)<sub>1.5</sub>, **2**).

Over the past few decades, metal-organic cages (MOCs) have attracted considerable attention because of their fascinating structures and properties.<sup>1–6</sup> In comparison to molecular recognition and separations, the MOCs-based catalysis has been relatively less studied.<sup>7,8</sup> As a discrete class of supramolecular complexes, they are usually polar organic solvents soluble without destruction of their structural integrity, so MOCs-based catalysis was normally in a homogeneous manner.<sup>9–14</sup> However, their recovery and reuse have been received much less attention. The development of recyclable and reusable MOC-based catalysts is of great significance in terms of atomic economy and eco-friendly issues.

In this contribution, we report for the first time a discrete Cu<sub>3</sub>L<sub>2</sub> MOC (**1**) by assembly of Cu(OAc)<sub>2</sub> and a new tripodal diketone ligand **L** in solution. **1** contains coordinatively unsaturated Cu(II) centres and can be a homogeneous catalyst to highly promote A<sup>3</sup>-coupling reaction in polar organic medium. Furthermore, **1** can be readily recovered from reaction solution by the addition of 1,4-dioxane via formation of the insoluble Cu(II)-MOF (**2**, Cu<sub>3</sub>L<sub>2</sub>·(1,4-dioxane)<sub>1.5</sub>) linked via Cu(II)-1,4-dioxane-Cu(II) linkage. This 1-to-2-to-1 process is reversible, so 1-based catalysis herein features a coordination interaction triggered homogeneous catalysis and heterogeneous recovery procedure.

College of Chemistry, Chemical Engineering and Materials Science, Collaborative Innovation Center of Functionalized Probes for Chemical Imaging in Universities of Shandong, Key Laboratory of Molecular and Nano Probes, Ministry of Education, Shandong Normal University, Jinan 250014, P. R. China. Email: yubindong@sdu.edu.cn.

Electronic Supplementary Information (ESI) available: Synthesis and characterization of **L**, **1** and **2**, single-crystal data, general procedure for the A<sup>3</sup>-coupling reaction catalysed by **1**, recycle of **1**, products characterization. See DOI: 10.1039/x0xx00000x

Scheme 1. Synthesis of **L**, **1** and **2**.

As shown in Scheme 1, tripodal ligand **L** with terminal diketone coordination sites was prepared by the coupling of 1,3,5-tribromobenzene with 3-acetylbenzeneboronic acid, and then a condensation reaction of the generated intermediate **A** and acetacetic ester in the presence of NaH in THF (79% yield, ESI<sup>+</sup>). **L** was assembled into Cu<sub>3</sub>L<sub>2</sub> (**1**) upon complexation with Cu(II) in CH<sub>2</sub>Cl<sub>2</sub> at room temperature with a molar ratio of 2:3 (88% yield, ESI<sup>+</sup>).

Electrospray ionization mass spectrometry (ESI-MS) provided substantial evidence for the formation of a Cu<sub>3</sub>L<sub>2</sub> species in solution. The MS spectrum (Fig. S3, ESI<sup>+</sup>) showed that the peak at *m/z* 1324.1137 was observed due to the formation of the [Cu<sub>3</sub>L<sub>2</sub>+Na<sup>+</sup>] species, thereby confirming that the Cu(II) ions in solution were chelated by three deprotonated ligand **L**.

The molecular structure of **1** was eventually determined by X-ray single-crystal analysis (CCDC 1848381, Tables S1 and S2, ESI<sup>+</sup>). As indicated in Fig. 1, **1** crystallized in the triclinic space group *P*-1. The Cu(II) centre in **1** lies in a quasi-square planar {CuO<sub>4</sub>} coordinated environment. Two twisted tripodal ligands **L** link three Cu(II) ions into an elliptical molecular cage, in which the Cu···Cu distances are in a range of 11.609 (24)–12.467 (21) Å. The distance between the opposite central phenyl rings is ca. 7 Å, while the longest distance between two opposite methyl groups is ca. 2.0 nm (Fig. 1). Besides X-ray single-crystal analysis, the observation of Cu 2p<sub>3/2</sub> peak at 934.3 eV in X-ray photoelectron spectroscopy (XPS) further confirmed that the copper ions in **1** were bivalent (Fig. S4, ESI<sup>+</sup>).<sup>15</sup> The existence of co-crystallized CH<sub>2</sub>Cl<sub>2</sub> solvent

## COMMUNICATION

## Journal Name

molecules was further confirmed by thermogravimetric analysis (TGA). The TGA result revealed that the observed solvent molecule weight loss is 16.5% (calculated 16.5% based on  $\text{Cu}_3\text{L}_2 \cdot 3\text{CH}_2\text{Cl}_2$ , Fig. S4, ESI<sup>†</sup>). Notably, **1** was very soluble in some organic solvents such as  $\text{CHCl}_3$ ,  $\text{CH}_2\text{Cl}_2$  and THF (Fig. S5, ESI<sup>†</sup>). In addition, the PXRD pattern performed on the as-synthesized sample is the same as that of simulated one, indicating that **1** was generated in a single phase (Fig. 2a). The formation of  $\text{Cu}_3\text{L}_2$  nanocage was further confirmed by dynamic light scattering (DLS) measurement (Fig. 2b). The observed dynamic diameter of **1** centred at ca. 2.2 nm, which is in good agreement with the TEM image (Fig. 2b) and single crystal analysis. The slight difference in size might be caused by the solvation effect depending on the different measurement.<sup>16</sup>

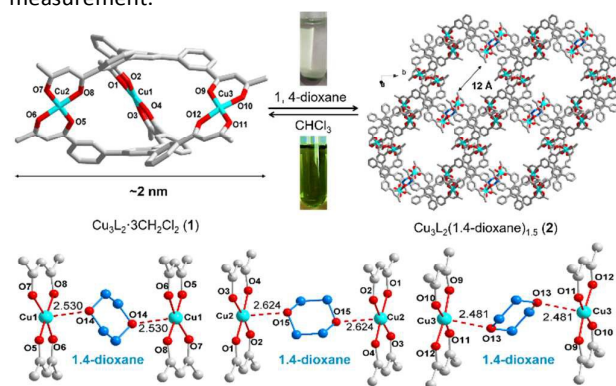


**Fig. 1** Reversible coordination-driven transformation between **1** and **2**. The X-ray single-crystal analysis revealed that **1** and **2** existed as the discrete metallacage and Cu(II)-MOF, respectively. The weak coordination bonds between 1,4-dioxane and Cu(II) centres in **2** are shown. The photographs showed that **1** was  $\text{CHCl}_3$ -soluble and **2** became insoluble upon addition of 1,4-dioxane in  $\text{CHCl}_3$ .

As mentioned above, the obtained  $\text{Cu}_3\text{L}_2$  metallacage contains three square-planar Cu(II) centres which are prone to bind small molecular donors at the axial coordination to form square pyramidal or octahedral coordination sphere.<sup>17</sup> Therefore, such a coordinated unsaturated metallacage was expected to be an ideal building block to construct polymeric network by the incorporation divergent bidentate coordination molecules such as 1,4-dioxane into polymeric backbone.<sup>18</sup>

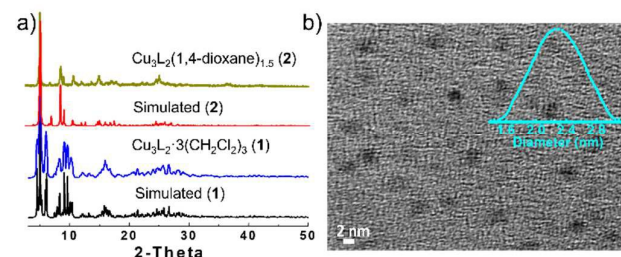


**Fig. 2** a) The simulated and measured PXRD patterns for **1** and **2**. b) TEM image and DLS measurement of **1**.

Following this idea, 1,4-dioxane was added to the  $\text{CHCl}_3$  solution of **1**, and the light green crystalline solids quantitatively precipitated (Fig. 1), indicating the formation of polymeric species. The X-ray single-crystal analysis (CCDC 1842443, Tables S1 and S2, ESI<sup>†</sup>) revealed that the formed

polymeric species of **2** crystallized in the monoclinic space group  $C2/c$ . As shown in Fig. 1, the  $\text{Cu}_3\text{L}_2$  cages were linked together by the involved 1,4-dioxane via three sets of weak Cu(II)···O bonds ( $d_{\text{Cu-O}} = 2.53(0)$ ,  $2.62(3)$  and  $2.48(3)$  Å, respectively) into a 2D network which contains the rounded pores with crystallographic diameter of ca. 12 Å. The measured PXRD pattern of **2** showed that it is distinctly different from that of **1**, but is identical to that of simulated one, demonstrating that **2** was obtained in pure phase (Fig. 2a).

The formation of **2** from **1** was further supported by their porosity difference based on the gas adsorption-desorption measurement (Fig. S6 and S7, ESI<sup>†</sup>).  $\text{N}_2$  adsorption at 77 K revealed absorption amounts of 87.48 and 125.74  $\text{cm}^3/\text{g}$  by **1** and **2**, respectively. Notably, no copper valence change was detected in **2** based on the XPS analysis (Fig. S8, ESI<sup>†</sup>).

It was noteworthy that **2** could dissociate in  $\text{CHCl}_3$  to regenerate **1**. Therefore, this 1-to-2-to-1 can be considered a reversible coordination interaction triggered dissolution-precipitation-dissolution process (Fig. 1). On the basis of this unique coordination-driven solubility, we expected that the 1-based homogeneous catalysis in  $\text{CHCl}_3$  and heterogeneous recovery with the aid of bidentate 1,4-dioxane donor should be achievable.

**Table 1.** Optimization of the model  $\text{A}^3$ -coupling reaction<sup>a</sup>

entry	T (°C)	solvent	<b>1</b> (mol%)	t (h)	yield (%) <sup>b</sup>
1	25	$\text{CHCl}_3$	3	24	98
2	25	$\text{CHCl}_3$	1	24	94
3	25	$\text{CHCl}_3$	0.3	24	84
4	25	THF	3	24	95
5	25	toluene	3	24	89
6	25	$\text{CH}_3\text{OH}$	3	24	57
7	25	$\text{CH}_3\text{CN}$	3	24	82
8	40	$\text{CHCl}_3$	3	2	53
9	50	$\text{CHCl}_3$	3	2	81
10	60	$\text{CHCl}_3$	3	2	98
11	25	$\text{CHCl}_3$	-	2	9
12	60	$\text{CHCl}_3$	-	2	13

<sup>a</sup> Reaction conditions: Under nitrogen, a mixture of benzaldehyde (0.5 mmol, 51  $\mu\text{L}$ ), phenylacetylene (0.75 mmol, 83  $\mu\text{L}$ ), pyrrolidine (0.60 mmol, 50  $\mu\text{L}$ ) and **1**. The coupling product was determined by <sup>1</sup>H NMR and MS spectra (Fig. S9, ESI<sup>†</sup>)<sup>b</sup> Yield was determined by the GC (Fig. S10, ESI<sup>†</sup>).

We initially examined the catalytic activity of **1** in this way by the  $\text{A}^3$ -coupling reaction, which is known as an important type of aldehyde-alkyne-amine one-pot multicomponent reaction. The obtained propargylamines are the important intermediates for the synthesis of various nitrogen-containing biologically active compounds.<sup>19</sup> Optimization of the reaction was first performed at different catalyst loading under room temperature to furnish the desired product in  $\text{CHCl}_3$  (Table 1, entries 1–3). The results indicated that this model  $\text{A}^3$ -coupling

reaction of benzaldehyde (**3**), pyrrolidine (**4**) with phenylacetylene (**5**) (molar ratio, 1.0:1.2:1.5) in the presence of **1** (3 mol%) proceeded very smoothly under room temperature to provide desired product of **6** (Fig. S9, ESI<sup>†</sup>) in excellent yield (98%) after 24h (Table 1, entry 1). When the reaction was conducted with a lower catalyst loading, 1 and 0.3 mol % instead of 3 mol %, the product of **6** was furnished in lower yields (Table 1, entries 2 and 3). Furthermore, when other kind of 1-soluble solvent such as THF was employed in the presence of 3 mol % **1**, the coupled product **6** was also obtained in excellent 95% yield (Table 1, entry 4). In contrast, the 1 poor soluble solvent such as toluene, MeOH and CH<sub>3</sub>CN were employed to give **6** in much lower yields (Table 1, entries 5-7) under the same reaction conditions, demonstrating that the efficiency of heterogeneous catalysis was indeed lower than that of corresponding homogeneous catalysis due to its inherent nature.

In addition, the reaction temperature appeared to be crucial to the catalytic efficiency. As shown in Table 1, upon increase of the reaction temperature from 25 to 60°C, the A<sup>3</sup>-coupling reaction rate was significantly enhanced (Fig. S11, ESI<sup>†</sup>). For example, 98% yield was achieved when the reaction was carried out at 60°C for only 2 h (Table 1, entries 8-10), and the corresponding turnover number (TON) and turnover frequency (TOF) values for the model reaction are 32.67 and 16.33 h<sup>-1</sup>, respectively. Without the aid of **1** (Table 1, entries 11-12), however, no significant conversion was observed at either 25°C (9% yield) or 60°C (13% yield), clearly denoting the catalytic activity of **1** herein.

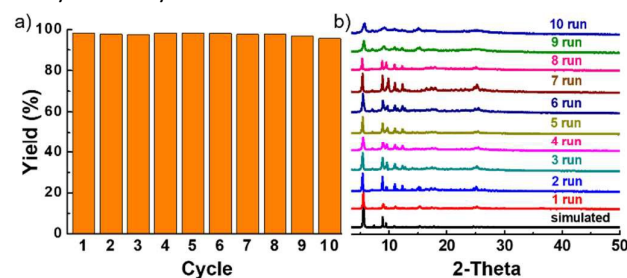
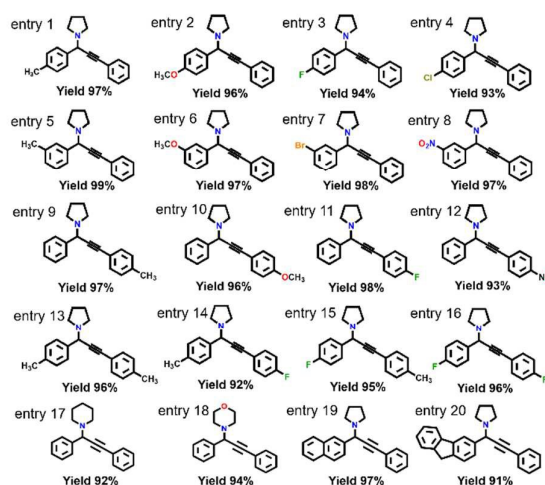


Fig. 3 a) 1-based catalytic cycle. b) The corresponding PXRD patterns of **2** after each catalytic run.

Once the reaction was finished, **1** could be readily separated from reaction system by coordination-driven solubility. Upon addition of 1,4-dioxane, **1** precipitated from reaction solution via formation of **2** (Fig. S12, ESI<sup>†</sup>), and the generated **2** could be resolvable in CHCl<sub>3</sub> and regenerated **1** which was directly used for the next catalytic run. Notably, **1** could be recycled at least 10 times in this way without loss of its catalytic activity under the optimized conditions (96 % yield for the tenth catalytic run, Fig. 3a and Fig. S13, ESI<sup>†</sup>). After ten catalytic runs, the PXRD patterns of **2** indicated that the structural integrity and crystallinity of **2** was still preserved, reflecting that **1** was stable during the multiple times repeatable A<sup>3</sup>-coupling catalytic process (Fig. 3b). On the other hand, **2** could also be directly used to promote this A<sup>3</sup>-coupling reaction in a heterogeneous way but with a lower catalytic efficiency.

Compared to the homogeneous case of **1**, the model reaction rate largely decreased with **2**. As indicated in Fig. S14 (ESI<sup>†</sup>), product **6** was generated in only 79% yield after 2 h at 60°C, and a longer time (4.5 h) was required to attain 93% yield. The difference in catalytic efficiency probably demonstrated the higher diffusion problem of the larger sized propargylamine to leave from the inner surface of the polymeric framework of **2**. This was not surprising if one considered that, for the reaction to proceed it was necessary that the three kinds of starting molecules had to encounter each other in the suitable orientation within the pores of **2**.

Table 2. A<sup>3</sup>-coupling reactions among various aldehydes, amines and alkynes catalysed by **1**<sup>a</sup>



<sup>a</sup> Reaction conditions: in nitrogen, aldehyde (0.5 mmol), alkyne (0.75 mmol), amine (0.60 mmol), **1** (3 mol%), CHCl<sub>3</sub> (1 mL), 60°C, 2h. Yields were determined by the GC (Fig. S15, ESI<sup>†</sup>).

With the above optimized reaction conditions in hand, we investigated the scope of this A<sup>3</sup>-coupling utilizing various substrates (Table 2). To our delight, **1** could be applicable to various functional groups such as -CH<sub>3</sub>, -NO<sub>2</sub>, -OCH<sub>3</sub>, -F, -Cl, and -Br (Table 2, entries 1-8, 93-99% yields) attached aldehydes. On the other hand, when phenylacetylene was replaced by other substituted aromatic alkynes, the reactions also proceeded very smoothly under the optimized conditions (Table 2, entries 9-16, 92-97% yields). In addition, when six-membered cyclic secondary amines such as piperidine (Table 2, entry 17, 92% yield) and 4-oxopiperidine (Table 2, entry 18, 94% yield) were used instead of pyrrolidine to perform the reactions, the expected products were also formed in excellent yields. Notably, the yields correspondingly decreased as the substrate size increased. As illustrated in Table 2, the coupling reactions for the desired products based on the naphthyl (Table 2, entry 19) and fluorenyl (Table 2, entry 20) substituted aldehydes were in excellent-to-good yields ranging from 97 to 91%, suggesting that the catalytic activity of **1** might result from the collaboration of internal and outside surface catalytic processes.

In contrast, the corresponding coupling product generated from fluorene-2-carboxaldehyde was obtained in only 71% yield with the aid of **2** in a heterogeneous way under the same reaction conditions (Fig. S16, ESI<sup>†</sup>), which further highlighted the homogeneous catalysis merit of **1**.

For understanding the mechanism of this novel Cu-cage promoted A<sup>3</sup>-reaction, we performed the ESI-MS measurement on the model reaction system. As shown in the spectra (Fig. S17, ESI<sup>†</sup>), the iminium cation of (I) from **3** and **4** was detected based on the observed peak at *m/z* 160.1140 (calcd for (C<sub>11</sub>H<sub>13</sub>N) M<sup>+</sup> *m/z* 160.1121). In addition, the peak at *m/z* 1404.2037 (calcd for (C<sub>80</sub>H<sub>60</sub>Cu<sub>3</sub>O<sub>12</sub>) [M+H]<sup>+</sup> *m/z* 1404.2046) indicated formation of the Cu(I)-acetylide adduct (II) from **5** and Cu<sub>3</sub>L<sub>2</sub> cage. These observations are consistent with the normally proposed A<sup>3</sup>-coupling reaction mechanism,<sup>20,21</sup> which involved the in situ generated iminium cation and the copper-activated Cu(I)-alkyne species. During the process, the {O<sub>4</sub>} coordination sphere might account for adequate electron delocalization to promise the reduction of Cu(II) to Cu(I), which was further promoted by the redox potential of Cu(II).<sup>22</sup> As shown in Fig. S18 (ESI<sup>†</sup>), the expected propargylamine **6** was finally generated, together with water and the regenerated **1**, by addition of the Cu(I)-acetylide to the iminium cation. Furthermore, the peak at *m/z* 1479.2755 for host-guest species of (C<sub>6</sub>H<sub>5</sub>CHO)(C<sub>4</sub>H<sub>8</sub>NH)@Cu<sub>3</sub>L<sub>2</sub> (calcd for (C<sub>83</sub>H<sub>70</sub>Cu<sub>3</sub>NO<sub>13</sub>) [M+H]<sup>+</sup> *m/z* 1479.2732) was also observed, implying that the Cu-cage herein served as not only a catalyst but also a kind of reaction vessel. As shown above, the smaller-sized substrates which could be readily encapsulated in the cage container would facilitate the coupling reactions. Interestingly, the ESI-MS results (Fig. S17, ESI<sup>†</sup>) also suggested a product-cage interaction, confirmed by observation of the peak assignable to **6**@Cu<sub>3</sub>L<sub>2</sub> (calcd for (C<sub>91</sub>H<sub>74</sub>Cu<sub>3</sub>NO<sub>12</sub>) [M+H]<sup>+</sup> *m/z* 1563.3103, found *m/z* 1563.3103).

In conclusion, we have reported, as the first of its kind, a novel Cu(II)-MOC that is a homogeneous catalyst and can highly promote the A<sup>3</sup>-coupling reaction to generate propargylamines with excellent yields and a reasonable scope. Its catalytic activity is comparable with the reported homogeneous Cu catalysts,<sup>23</sup> but showed a better catalytic performance than those of copper-based heterogeneous catalysts (Table S3, ESI<sup>†</sup>). More importantly, it featured an interesting coordination-driven solubility and could be recycled at least ten times without loss its activity, which was the advantage of solid catalysts such as Cu-MOFs.<sup>24</sup> This reversible coordination interaction triggered homogeneous catalysis and heterogeneous recovery might open up new avenues for the design and synthesis of new type of catalysts with both homo- and heterogeneous catalyst merits.<sup>25</sup>

## Conflicts of interest

There are no conflicts to declare.

## Acknowledgements

We are grateful for financial support from NSFC (Grant Nos. 21671122, 21475078, 21301109), Taishan scholar's construction project and Shandong Provincial Natural Science Foundation (No. ZR2018MB005).

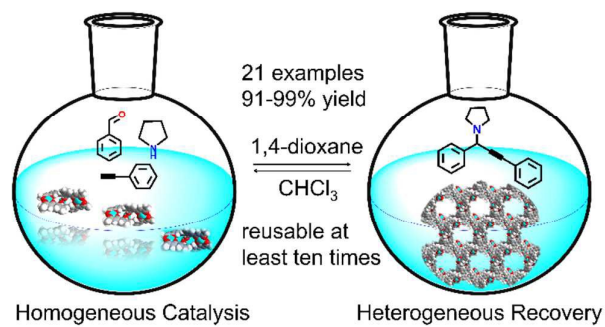
## Notes and references

1. T. R. Cook, Y.-R. Zheng, P. J. Stang, *Chem. Rev.*, 2013, **113**, 734–777.
2. M. D. Pluth, R. G. Bergman, K. N. Raymond, *Acc. Chem. Res.*, 2009, **42**, 1650–1659.
3. T. R. Cook, P. J. Stang, *Chem. Rev.*, 2015, **115**, 7001–7045.
4. C.-Y. Su, Y.-P. Cai, C.-L. Chen, M. D. Smith, W. Kaim, H.-C. zur Loye, *J. Am. Chem. Soc.*, 2003, **125**, 8595–8613.
5. Y.-B. Dong, P. Wang, J. Ma, X.-X. Zhao, H.-Y. Wang, B. Tang, R.-Q. Huang, *J. Am. Chem. Soc.*, 2007, **129**, 4872–4873.
6. W. Zhang, D. Yang, J. Zhao, L. Hou, J. L. Sessler, X.-J. Yang, B. Wu, *J. Am. Chem. Soc.*, 2018, **140**, 5248–5256.
7. H. Amouri, C. Desmarets, J. Moussa, *Chem. Rev.*, 2012, **112**, 2015–2041.
8. C. J. Brown, F. D. Toste, R. G. Bergman, K. N. Raymond, *Chem. Rev.*, 2015, **115**, 3012–3035.
9. W. Cullen, A. J. Metherell, A. B. Wragg, C. G. P. Taylor, N. H. Williams, M. D. Ward, *J. Am. Chem. Soc.*, 2018, **140**, 2821–2828.
10. T. H. Noh, E. Heo, K. H. Park, O.-S. Jung, *J. Am. Chem. Soc.*, 2011, **133**, 1236–1239.
11. P. F. Kuijpers, M. Otte, M. Dürr, I. Ivanovic-Burmazović, J. N. H. Reek, B. de Bruin, *ACS Catal.*, 2016, **6**, 3106–3112.
12. L.-X. Cai, S.-C. Li, D.-N. Yan, L.-P. Zhou, F. Guo, Q.-F. Sun, *J. Am. Chem. Soc.*, 2018, **140**, 4869–4876.
13. G. Tan, Y. Yang, C. Chu, H. Zhu, H. W. Roesky, *J. Am. Chem. Soc.*, 2010, **132**, 12231–12233.
14. Q.-T. He, X.-P. Li, L.-F. Chen, L. Zhang, W. Wang, C.-Y. Su, *ACS Catal.*, 2013, **3**, 1–9.
15. J.-P. Ma, S.-Q. Wang, C.-W. Zhao, Y. Yu, Y.-B. Dong, *Chem. Mater.*, 2015, **27**, 3805–3808.
16. C.-W. Zhao, J.-P. Ma, Q.-K. Liu, Y. Yu, P. Wang, Y.-A. Li, K. Wang, Y.-B. Dong, *Green Chem.*, 2013, **15**, 3150–3154.
17. Y.-B. Dong, M. D. Smith, H.-C. zur Loye, *Inorg. Chem.*, 2000, **39**, 1943–1949.
18. V. Calvo-Pérez, S. Ostrovsky, A. Vega, J. Pelikan, E. Spodine, W. Haase, *Inorg. Chem.*, 2006, **45**, 644–649.
19. K. Lauder, A. Toscani, N. Scalacci, D. Castagnolo, *Chem. Rev.*, 2017, **117**, 14091–14200.
20. M. Gopiraman, D. Deng, S. G. Babu, T. Hayashi, R. Karvembu, I. S. Kim, *ACS Sustainable Chem. Eng.*, 2015, **3**, 2478–2488.
21. U. C. Rajesh, U. Gulati, D. S. Rawat, *ACS Sustainable Chem. Eng.*, 2016, **4**, 3409–3419.
22. E. Loukopoulou, M. Kallitsakis, N. Tsoareas, A. Abdul-Sada, N. F. Chilton, I. N. Lykakis, G. E. Kostakis, *Inorg. Chem.*, 2017, **56**, 4898–4910.
23. C. Zhao, D. Seidel, *J. Am. Chem. Soc.*, 2015, **137**, 4650–4653.
24. I. Luz, F. X. L. i Xamena, A. Corma, *J. Catal.*, 2012, **285**, 285–291.
25. Y. Li, Y. Dong, Y.-L. Wei, J.-J. Jv, Y.-Q. Chen, J.-P. Ma, J.-J. Yao, Y.-B. Dong, *Organometallics*, 2018, **37**, 1645–1648.

## Journal Name

## COMMUNICATION

For table content



A novel Cu<sub>3</sub>L<sub>2</sub> metal-organic cage, which features the coordination interaction triggered solubility, can be a highly active and reusable catalyst to homogeneously catalyse the one-pot aldehyde-alkyne-amine A<sup>3</sup>-coupling reaction.